Radio Frequency Current Density Imaging with A 180° Sample Rotation

Dinghui Wang, Michael L.G. Joy, Weijing Ma, Tim P. DeMonte and Adrian I. Nachman

Outline

- Introduction
- RF-CDI with a single 180-degree rotation
- Three-dimensional RF current density reconstruction
- Discussion and conclusions

Basic (circa 1980) ideas behind CDI methods

- Allow imaging of the electrical aspects of living tissues and organs.
- Use MRI to acquire internal measurements of Magnetic fields permitting better tomography than EIT.
- Make full use of Maxwell's equations to allow quantitative imaging.

Current Density Imaging (CDI)

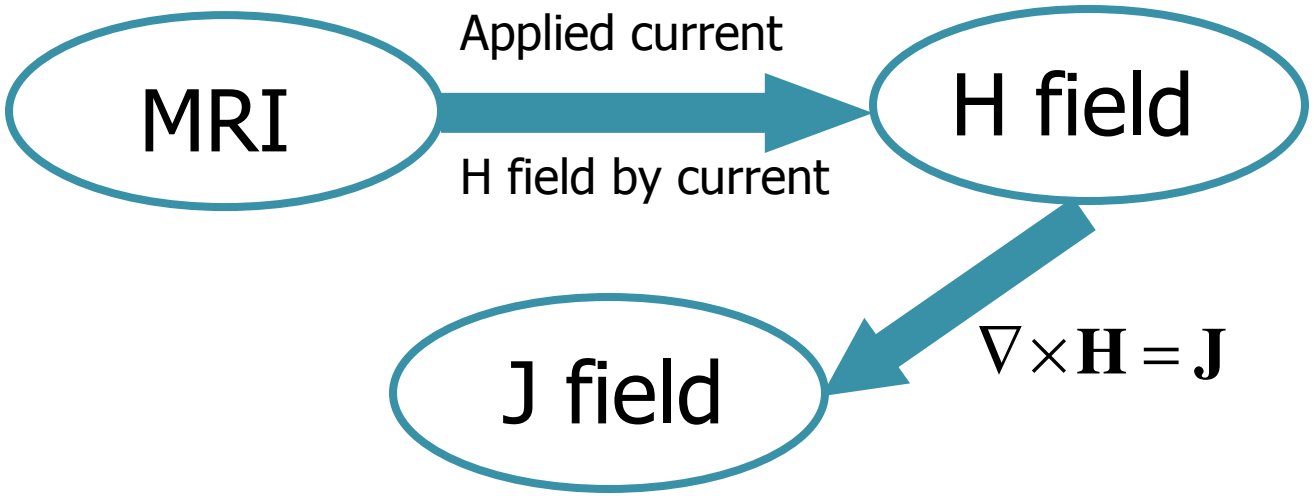

- Low frequency CDI (LF-CDI)
  up to 100 Hz
- Radio frequency CDI (RF-CDI)
  the Larmor frequency, 5-300 MHz

Current Density Impedance Imaging (CDII)

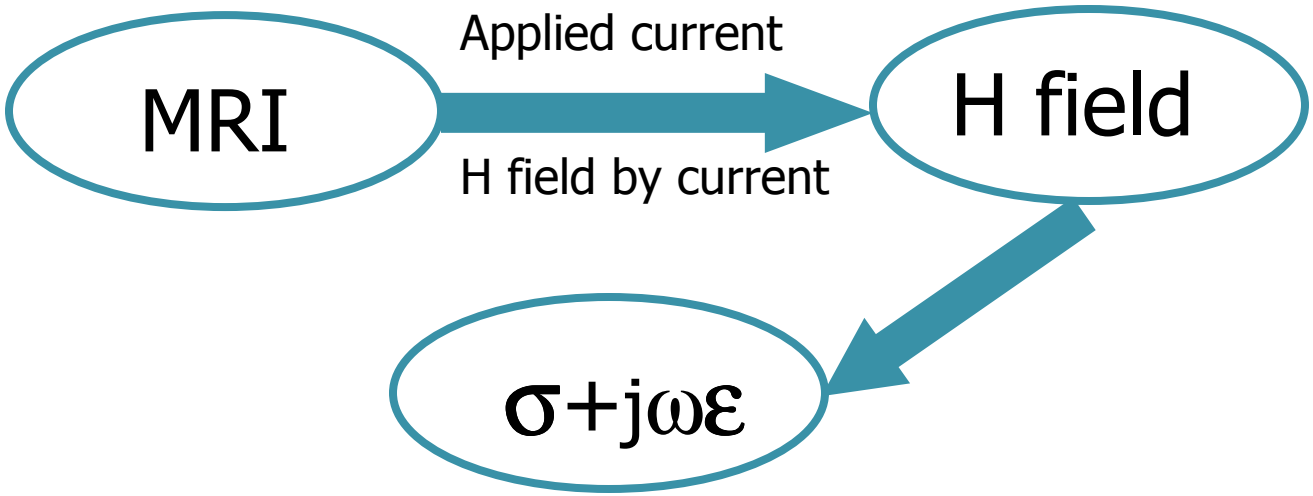

- Low frequency CDI (LF-CDI)
  up to 100 Hz
- Radio frequency CDI (RF-CDI)
  the Larmor frequency, 5-300 MHz

Biomedical Applications of CDI

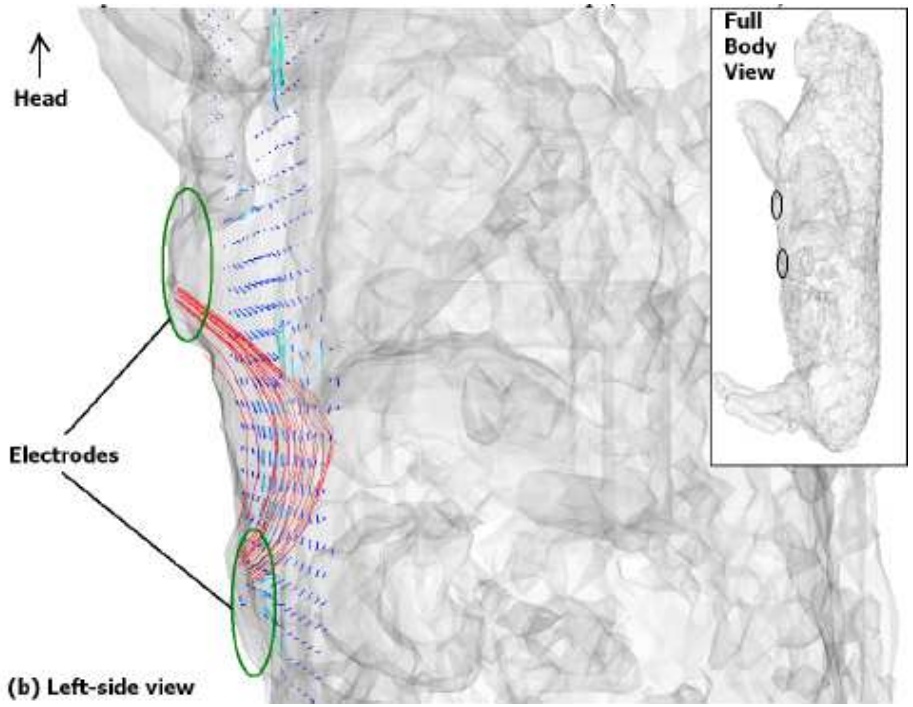

- LF-CDI on live pig

Why RF-CDI ?

- Higher current can be tolerated without nerve and muscle stimulation.
  - More applications. Less noise.
- Dielectric properties measurable.
- Induced currents eliminate electrode tissue interface issues.

Limitations of Previous RF-CDI Reconstruction

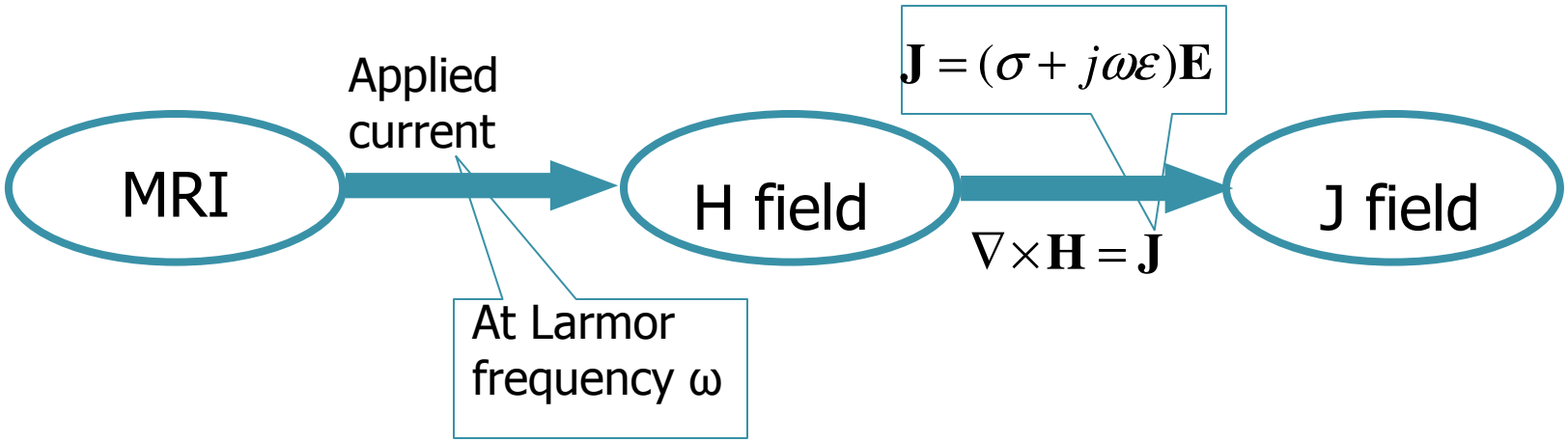

Only compute J_z

Single orientation approximation

What is Measured

- Transverse magnetic field

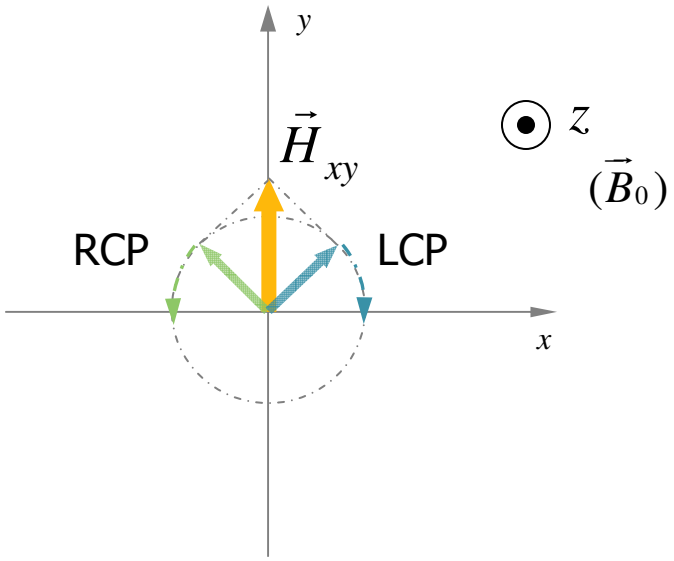

LCP: Left Circularly Polarized

RCP: Right Circularly Polarized

- Only LCP component can be measured

Single Orientation Reconstruction

$$J_z = \frac{\partial H_y}{\partial x} - \frac{\partial H_x}{\partial y} = j\left(\frac{\partial H_L}{\partial x} - \frac{\partial H_R}{\partial x}\right) - \left(\frac{\partial H_L}{\partial y} + \frac{\partial H_R}{\partial y}\right)$$

$$H_L \sim \underbrace{(\tilde{H}_x, \tilde{H}_y)}_{\text{LCP}} \neq (H_x, H_y) \xrightarrow{\ ?\ } J_z$$

$$\nabla \cdot \mathbf{H} = 0 \Rightarrow J_z = 2j\frac{\partial H_L}{\partial x} - 2\frac{\partial H_L}{\partial y} + j\frac{\partial H_z}{\partial z}$$

- Single orientation approximation

$$\left|\partial H_z / \partial z\right| << \left|J_z\right|$$

Single Orientation Approximation - Theoretical Implication

$$J_z = 2j\frac{\partial H_L}{\partial x} - 2\frac{\partial H_L}{\partial y} + j\frac{\partial H_z}{\partial z}$$

Ideally, $\frac{\partial H_z}{\partial z} = 0 \Rightarrow \frac{\partial H_x}{\partial x} + \frac{\partial H_y}{\partial y} = 0$

$$\mathbf{H} = \mathbf{H}_1 + \mathbf{H}_2$$

$$\mathbf{H}_1 = H_z\vec{a}_z \qquad \mathbf{H}_2 = H_x\vec{a}_x + H_y\vec{a}_y$$

Single Orientation Approximation - Impact on Practice

- Validity cannot be examined by measured data
- A sufficient condition– current flow globally in z direction $(\mathbf{H}_1 = H_z \vec{a}_z = 0)$
- May easily be violated in biomedical applications

Reconstruction with a Sample Rotation

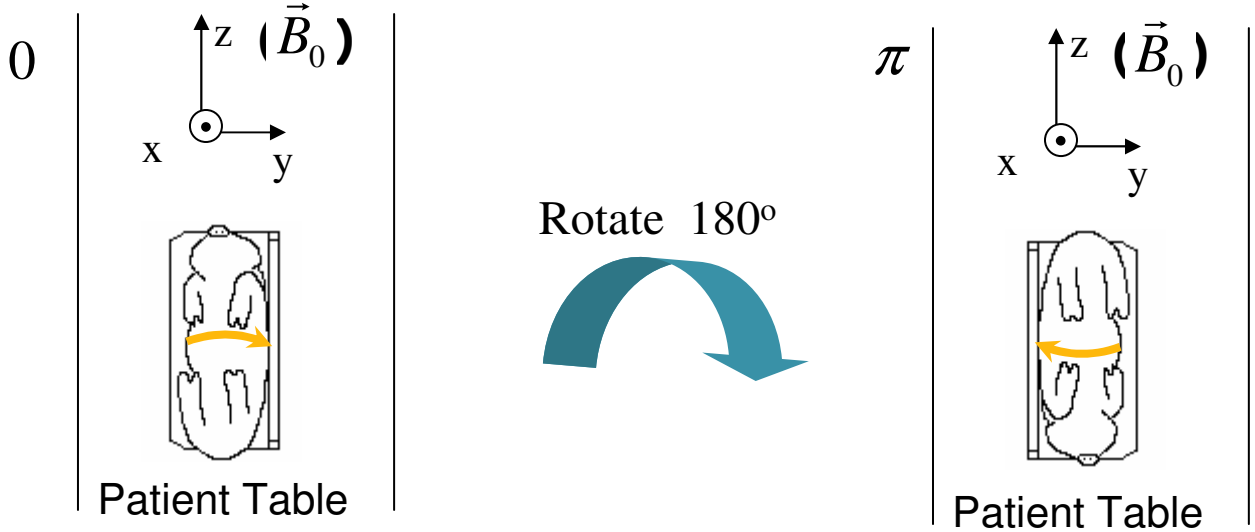

$$+ \begin{matrix} (\tilde{H}_x^0, \tilde{H}_y^0) \\ (\tilde{H}_x^\pi, \tilde{H}_y^\pi) \end{matrix} \longrightarrow (H_x, H_y) \longrightarrow J_z$$

LCP

RCP

Simulation Verification

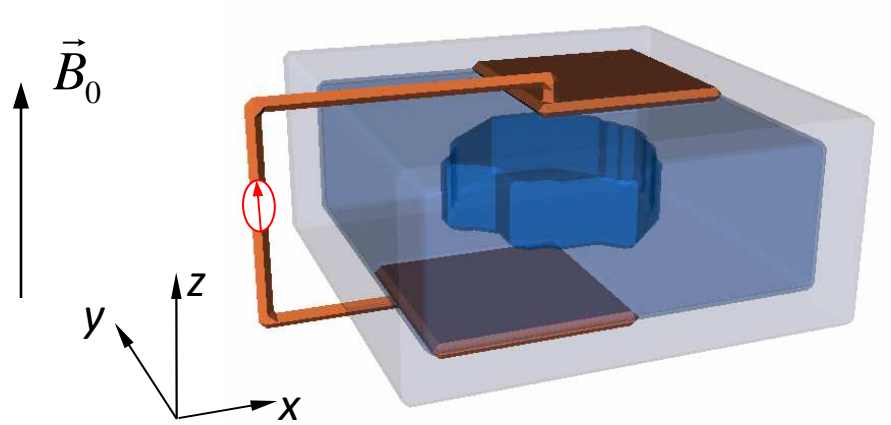

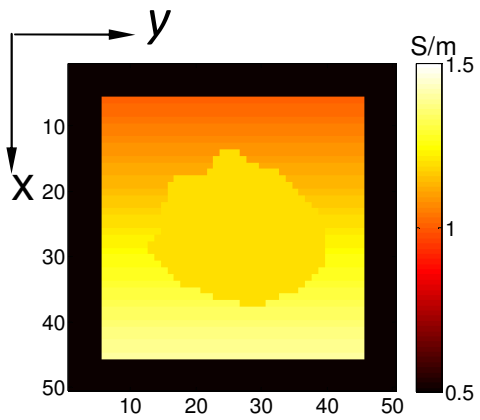

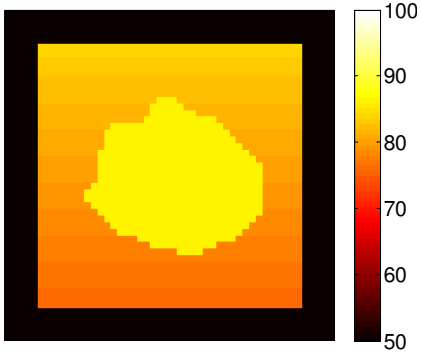

Results

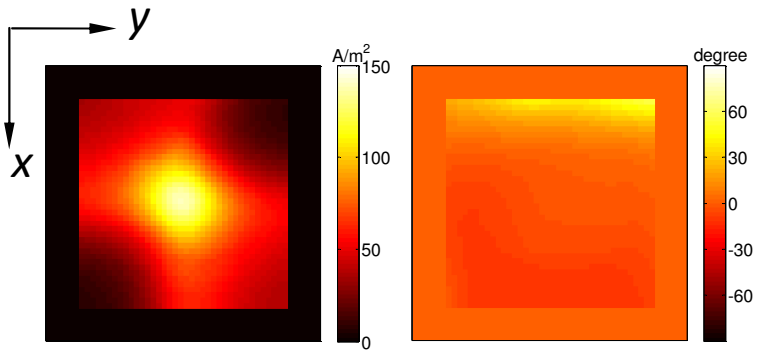

Forwarding modeling

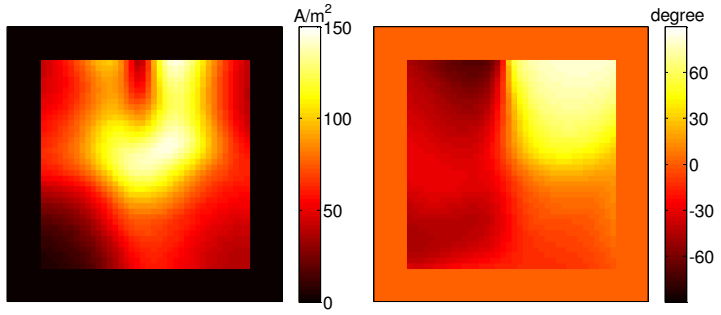

Method 1

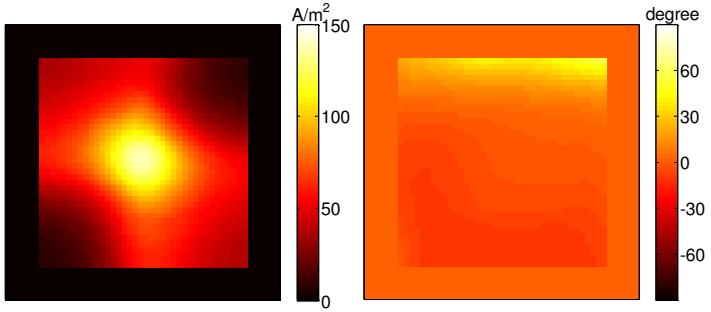

Method 2

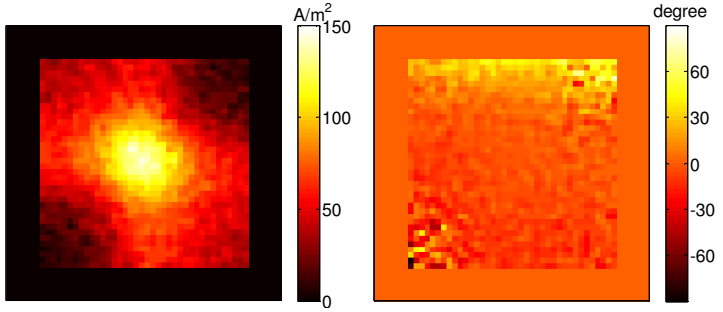

Method 2 with noise

Method 1: single orientation

Method 2: 180° rotation

Experimental Testing

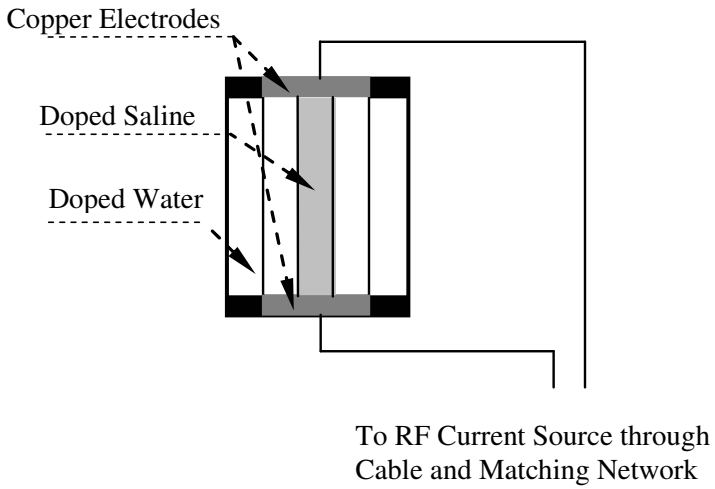

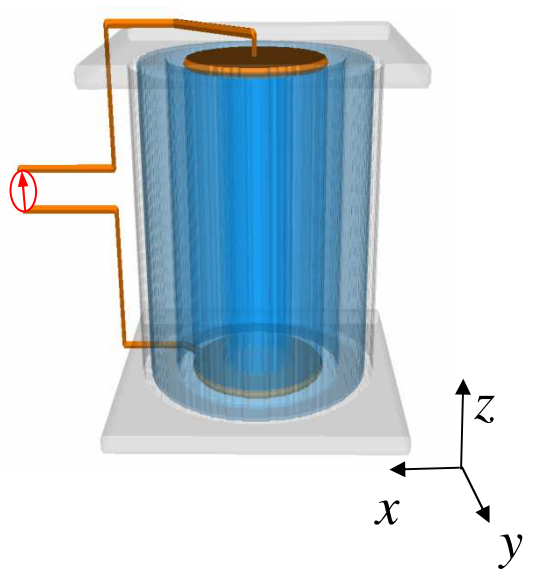

Experiment 1

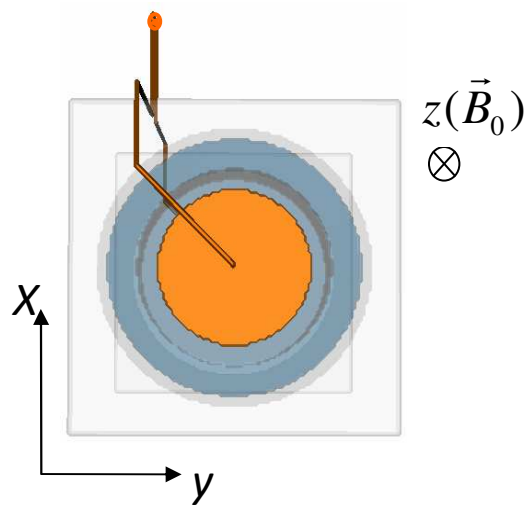

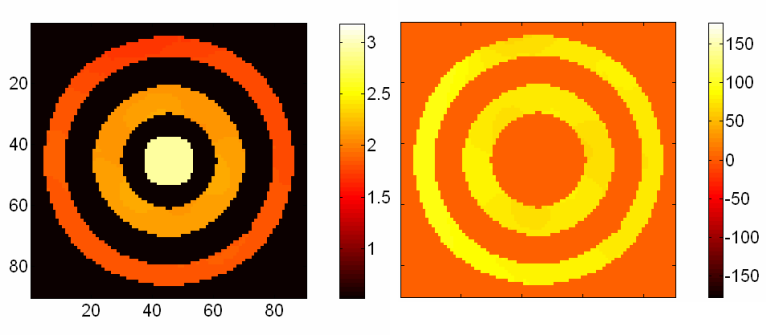

Forwarding modeling

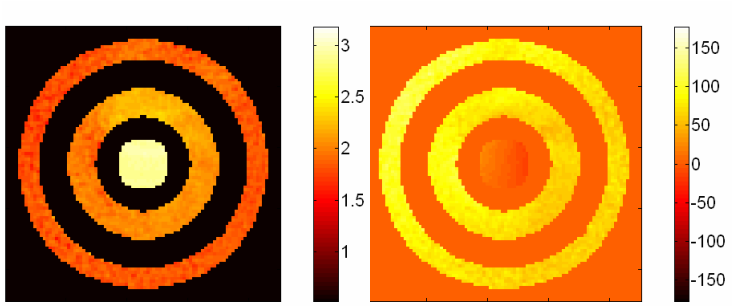

Method 1

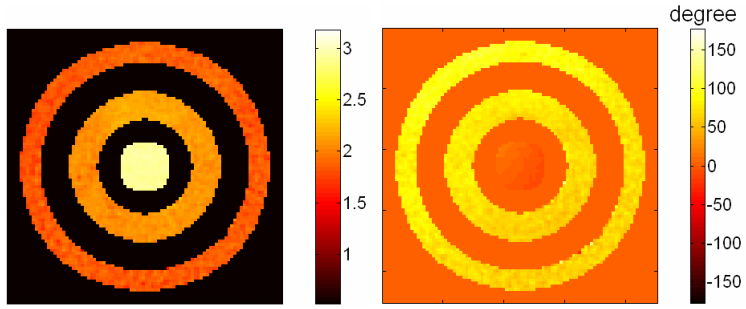

Method 2

Method 1: single orientation

Method 2: 180° rotation

Experiment 2

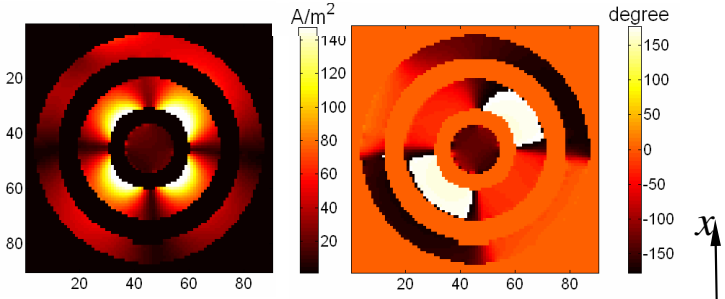

Predicted error of method 1

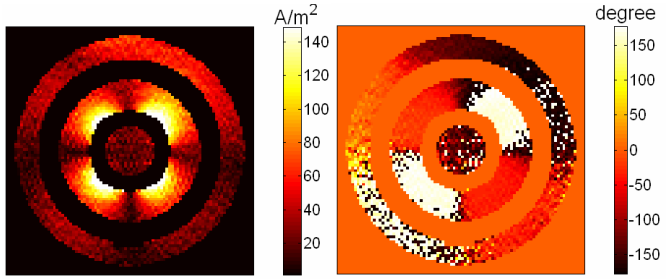

Method 1

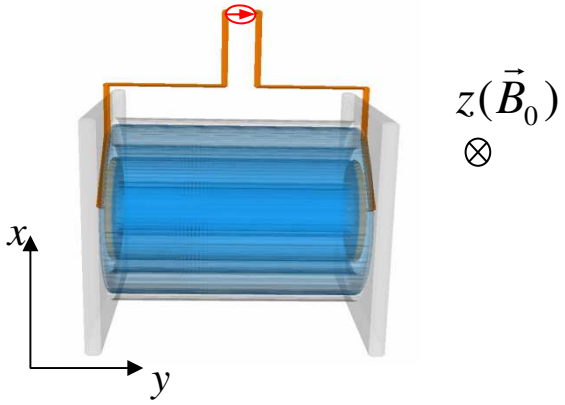

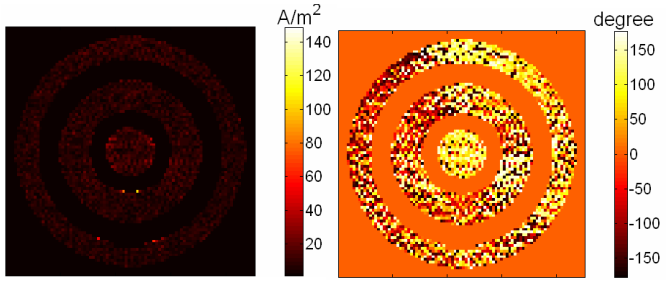

Method 2

Method 1: single orientation

J_z has significant error

Method 2: 180° rotation

J_z is close to the correct value

RF Current Density Vector Reconstruction -Three or Four Sample Positions

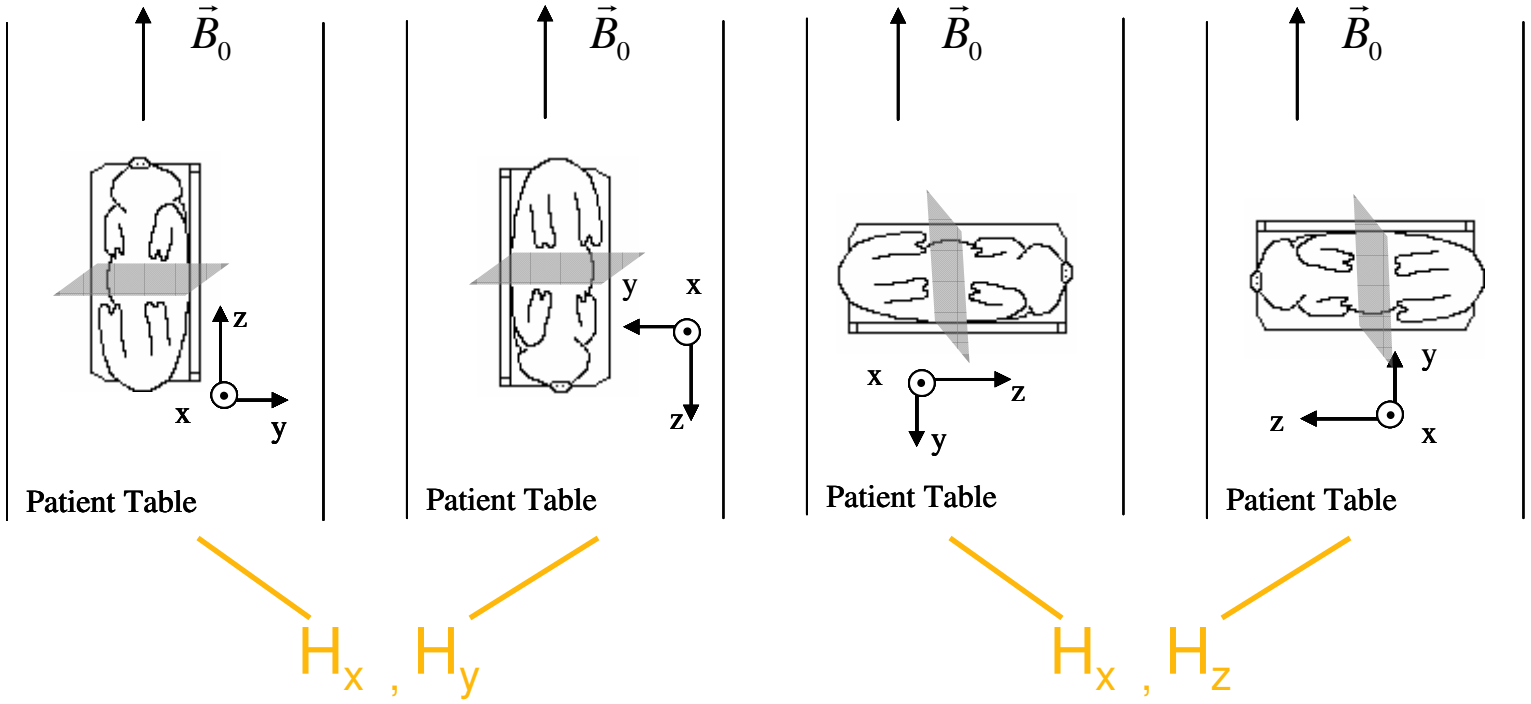

Simulation Verification

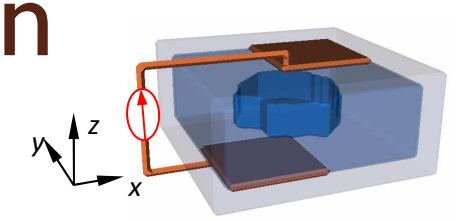

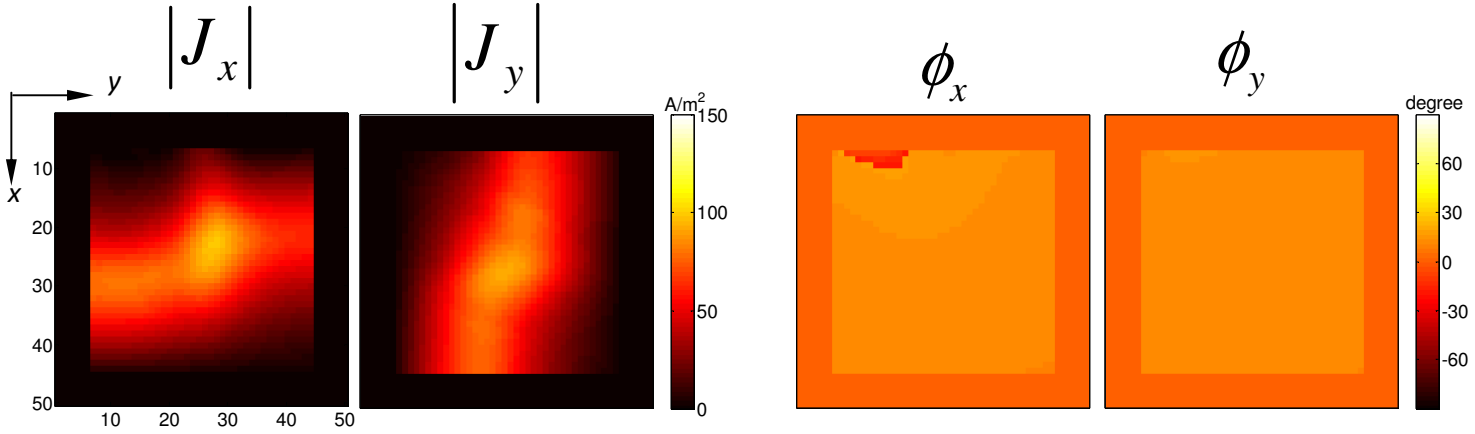

Forwarding modeling

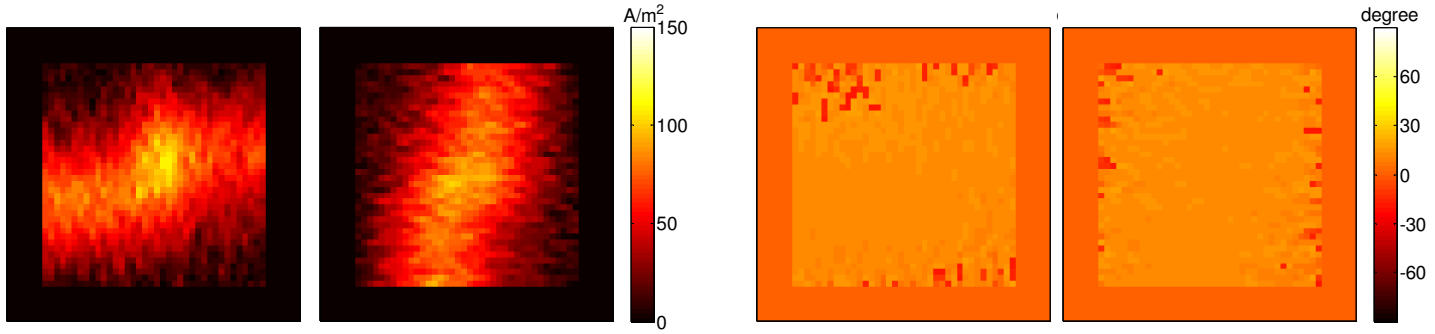

Reconstruction with added noise

Experimental Testing

Simulation

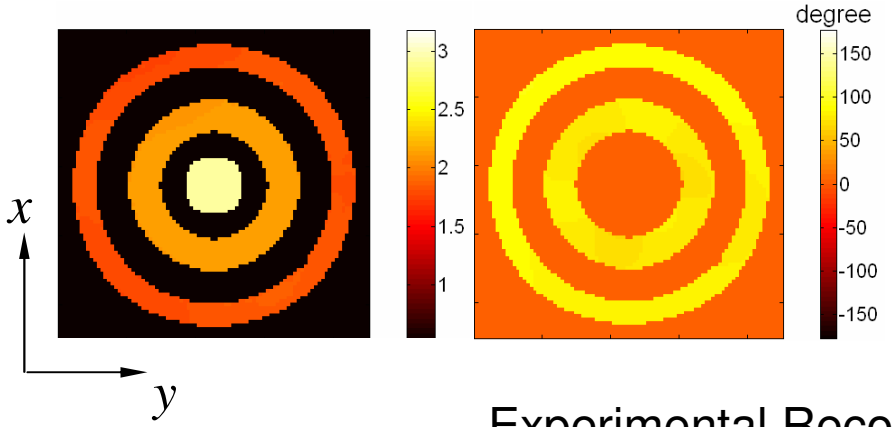

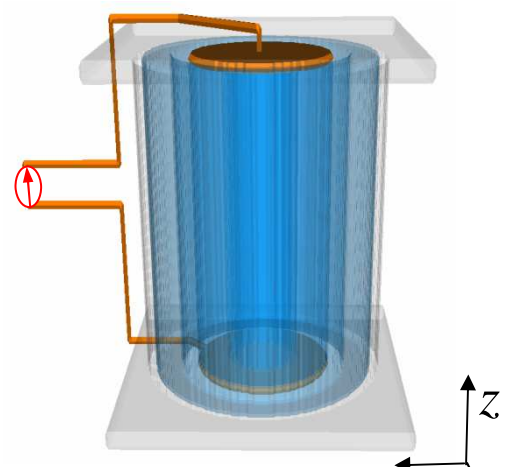

Experimental Reconstruction

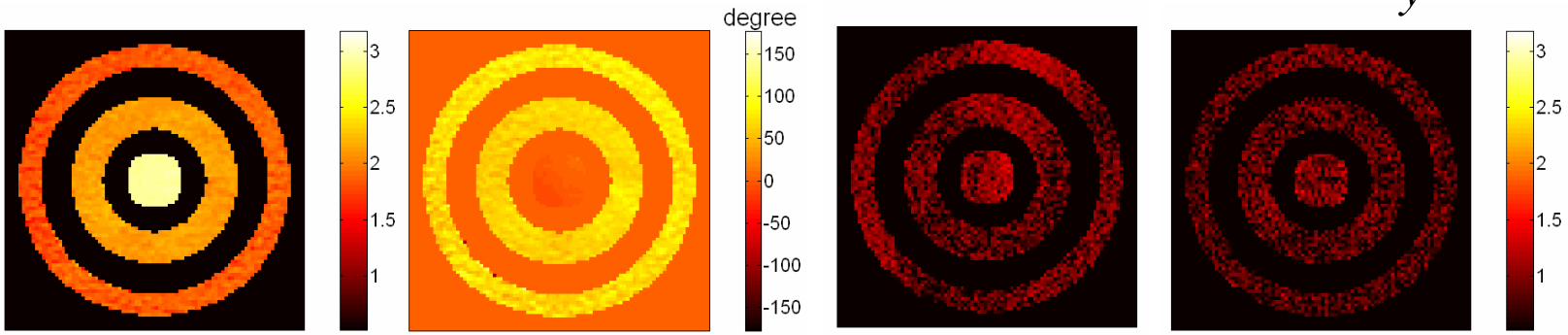

$|J_z|$ ϕ_z $|J_x|$ $|J_y|$

Comparison of the Results

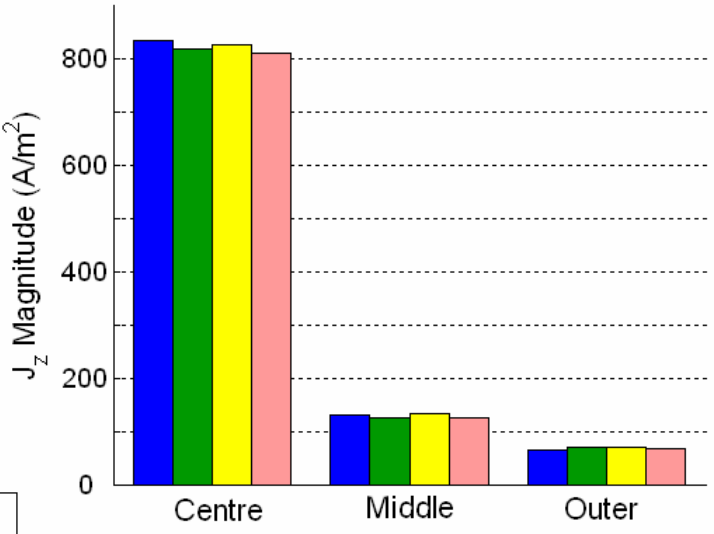

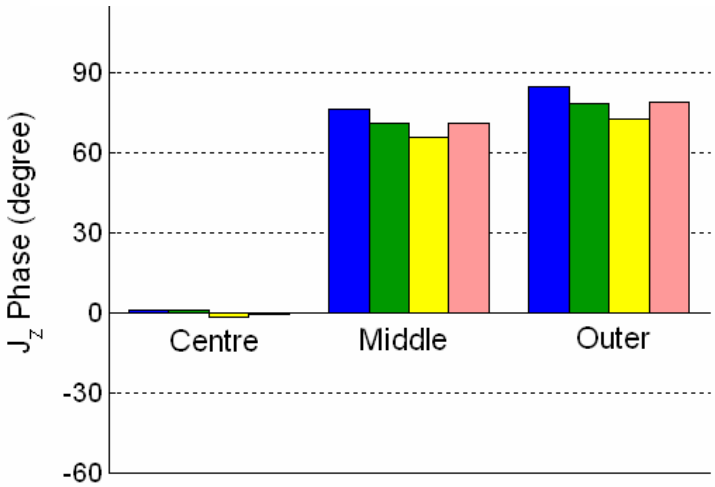

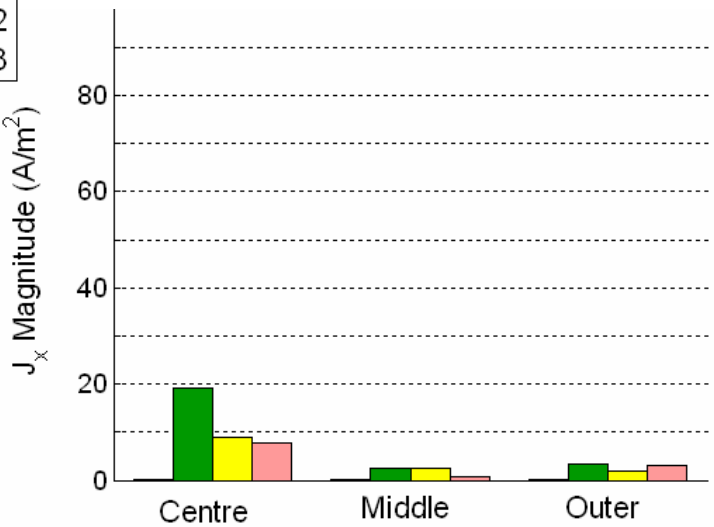

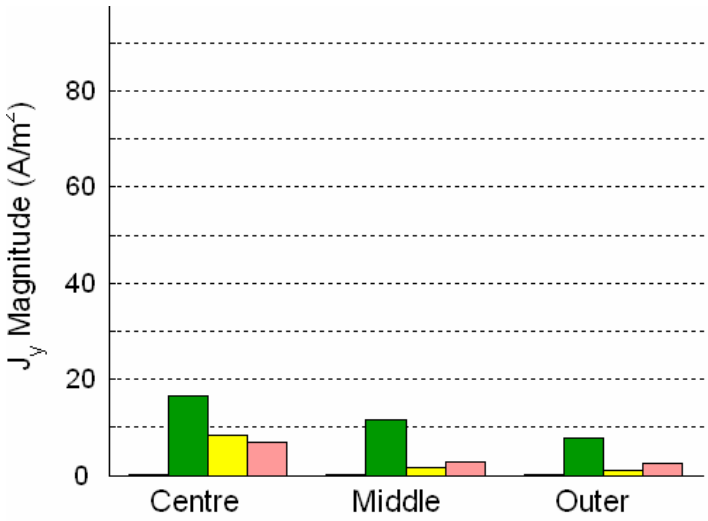

Discussion

- Imaging conditions

  Uniformity of the direction of B_1

- Practical consideration for sample rotations

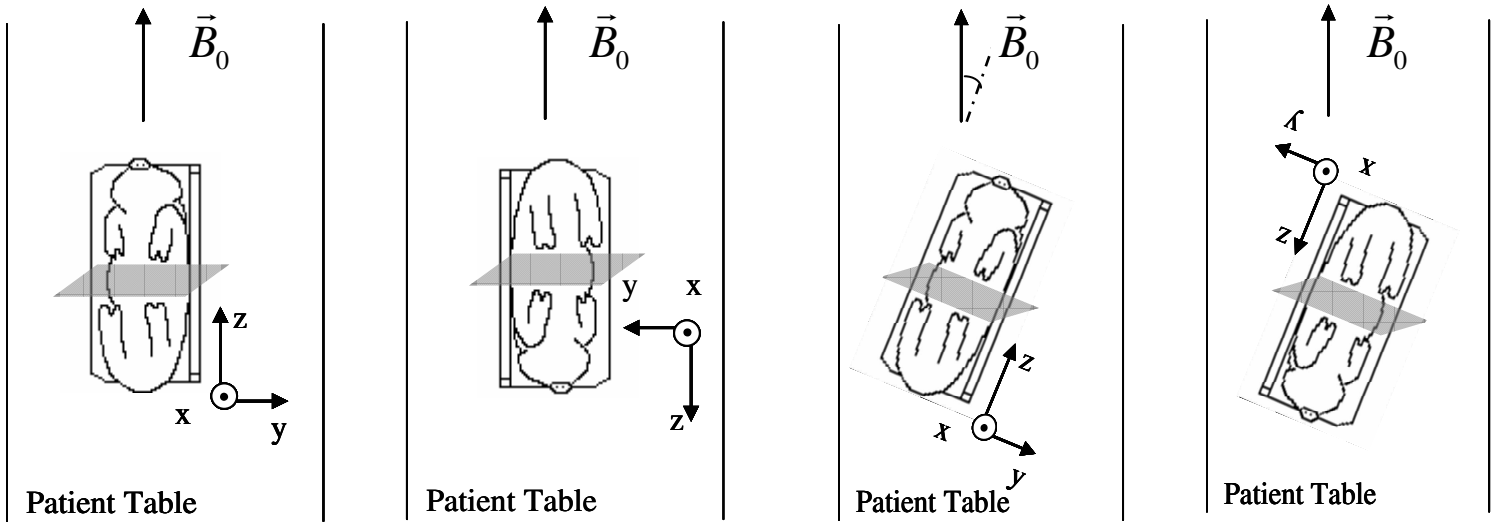

Towards RF Impedance Imaging

- Significance
- Possible computation methods

$$\gamma = \sigma + j\omega\varepsilon = -j\frac{\left(\nabla^2\mathbf{H}\right)\cdot\left(\nabla\times\mathbf{H}\right)}{\omega\mu_0\mathbf{H}\cdot\left(\nabla\times\mathbf{H}\right)}$$

Conclusions

- We have demonstrated for the first time that all three components of RF current density vector can be reconstructed.
- The work presented in this thesis is expected to significantly enhance RF-CDI to image biological subjects.

Acknowledgements

- Dr. Greig Scott
- Ning Zhang, Emidio Tarulli
- MITACS, NSERC, OGS & OGSST

Why RF-CDI

- Higher current can be tolerated without nerve and muscle stimulation.

  More applicable in biomedical applications
  Higher current means less noisy images

- Working at different frequency range, RF-CDI may reveal new information about tissues.